

DiffGen: Robot Demonstration Generation via Differentiable Physics Simulation, Differentiable Rendering, and Vision-Language Model

Yang Jin^{2*}, Jun Lv^{1*}, Shuqiang Jiang^{2,3†}, Cewu Lu^{1†}

Abstract—Generating robot demonstrations through simulation is widely recognized as an effective way to scale up robot data. Previous work often trained reinforcement learning agents to generate expert policies, but this approach lacks sample efficiency. Recently, a line of work has attempted to generate robot demonstrations via differentiable simulation, which is promising but heavily relies on reward design, a labor-intensive process. In this paper, we propose DiffGen, a novel framework that integrates differentiable physics simulation, differentiable rendering, and a vision-language model to enable automatic and efficient generation of robot demonstrations. Given a simulated robot manipulation scenario and a natural language instruction, DiffGen can generate realistic robot demonstrations by minimizing the distance between the embedding of the language instruction and the embedding of the simulated observation after manipulation. The embeddings are obtained from the vision-language model, and the optimization is achieved by calculating and descending gradients through the differentiable simulation, differentiable rendering, and vision-language model components, thereby accomplishing the specified task. Experiments demonstrate that with DiffGen, we could efficiently and effectively generate robot data with minimal human effort or training time.

I. INTRODUCTION

With the development of deep learning, significant success has been achieved in the fields of computer vision [13, 14, 22], language modeling [1, 6, 41, 48], and context generation [7, 11, 45]. Behind this progress, data has always played a key role. In recent years, researchers have showcased robots’ capacity to acquire manipulation policies from demonstration data. By utilizing techniques like imitation learning [15, 35], robots can effectively learn specific skills from these demonstrations. Scaling up the training data to encompass a variety of skills becomes a crucial next step in developing robot systems capable of performing diverse tasks in the physical world at the human level. Given the costliness of collecting real-world robot manipulation data, significant focus has been placed on generating such data in simulators [20, 33, 36, 49, 50, 52].

There are two key steps in simulated robot manipulation data generation: scene construction and expert trajectory generation. With the advancement of generative artificial intelligence technique, automatic scene construction [20, 49, 50] can be achieved by utilizing large language models [1] to generate scene descriptions and mesh generation models [26] to create objects for the scene. In previous work, given a well-constructed task scene, the most popular approach is to train a policy via reinforcement learning to rollout manipulation

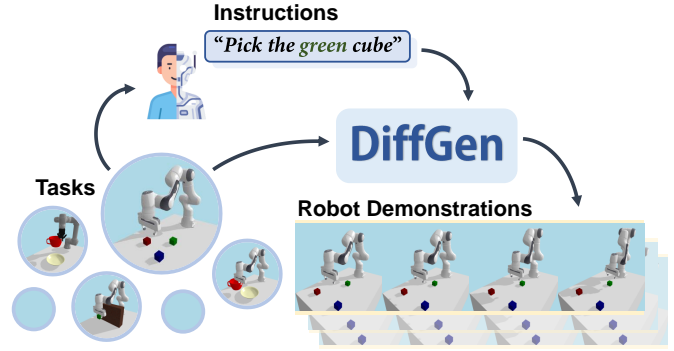


Fig. 1. With DiffGen, we could automatically and efficiently generate robot demonstrations, given simulated task environments and text-based instructions.

trajectories [33, 46, 50]. However, model-free reinforcement learning is criticized for its lack of sample efficiency and interpretability. To address this, a line of work is demonstrating the potential to utilize differentiable simulation to generate robot manipulation trajectories more efficiently and effectively [23, 25, 28, 29, 42, 57]. To optimize the manipulation action, most approaches still rely on reward design by engineers, which is labor-intensive and hard to scale up. As shown in Fig. 1, in this paper, we are aiming to develop a novel system DiffGen to achieve automatic and efficient simulated robot demonstration generation by integrating differentiable physics simulation [4, 5, 16, 51], differentiable rendering [24, 56] and vision-language pretrained model [32, 41, 46].

With differentiable physics simulation and rendering, visual observations can be generated to reflect the state change after robot manipulation. Previous works [19, 29, 30] have attempted to integrate them to address system or state identification problems. Inspired by recent progress in visual representation learning [2, 10, 37] and multi-modal learning [17, 32, 41, 46], our insight is that the integration of simulation, rendering, and cross-modal learning could effectively model the mapping between action and state, state and observation, and observation and instruction. By making all components differentiable, we can seamlessly connect each module and determine the mapping from task instructions to robot control signals, which will enable efficient robot demonstration generation.

Specifically, when given a manipulation scenario and a text-based task instruction, the system initiates the robot action sequence to control the robot in the differentiable physics simulation. Subsequently, by leveraging differentiable rendering,

*Equal contribution

†Equal advising

¹Shanghai Jiao Tong University, ²University of Chinese Academy of Sciences, ³Institute of Computing Technology, Chinese Academy of Sciences

observation images are produced to depict the scene’s state after the robot manipulation. A pretrained vision-language model is then utilized to evaluate the discrepancy between the image-based observation and the text-based task instruction, thereby serving as the objective function to guide the robot in completing the task. Thanks to the differentiability of the physics simulation, rendering, and the vision-language model, the system can directly explore feasible action sequences to execute the manipulation task in alignment with the task instruction, employing optimization-based methods such as gradient descent. Finally, simulated robot manipulation demonstration data is generated.

To evaluate the performance of our proposed system, we conducted several experiments. The results demonstrate that our system can generate simulated manipulation demonstrations for three different scenarios with distinct text-based task instructions. The proposed system exhibits better efficiency compared to reinforcement learning methods employing hand-crafted reward functions or reward functions generated by large language models.

The main contribution is summarized as follows:

- We introduce a language-guided framework aimed at efficiently generating robot demonstrations.
- We integrate differentiable simulation, differentiable rendering, and a pretrained vision-language model to facilitate manipulation trajectory generation in simulation.
- We conduct experiments demonstrating the superior efficiency and reduced human effort of our new paradigm, compared with existing methods.

II. RELATED WORK

In this section, we provide a review of the literature related to the key components of our approach, including the generation of robot demonstration, integration of differentiable physics-based simulation and rendering, and reward learning. We also explain how our approach differs from previous works in these areas.

A. Robot Demonstration Generation

Robotics researchers have developed many different kinds of physics-based simulators [8, 34, 47, 51, 52] in the past and employed these simulators for robot demonstration generation. A burdensome aspect of using simulators is that it always requires engineers to build scenes for different tasks. However, with recent progress in generative artificial intelligence, such as large language models [1] and mesh generation [26, 39] from images or text, a line of work is aiming to build generative simulators to scale up robot demonstration generation. For instance, Wang et al. [50], Wang et al. [49], and Katara et al. [20] utilize large language models to automatically generate task descriptions and build the corresponding simulation environments. Additionally, Lv et al. [28] constructs simulation environments from the real world and generates robot demonstrations within the simulation. Mandlekar et al. [36] can generate large-scale robot data by augmenting human demonstrations. Our work focuses on how to generate robot

demonstrations in specific task scenarios based on text-based instructions from humans or intelligent agents.

B. Integration of Differentiable Physics-based Simulation and Rendering

Physics simulations and renderers are essential tools in the domains of robotics and computer graphics. Recently, significant advancements have been achieved in the fields of differentiable physics simulation [4, 5, 8, 16, 40, 51, 54] and differentiable rendering [21, 24, 27, 56]. Jatavallabhula et al. [19] proposed a system that utilizes differentiable simulation and rendering to achieve system identification. In a similar vein, Ma et al. [30] leverage differentiable simulation and rendering for cross-domain parameter estimation from video. Additionally, Lv et al. [29] integrated differentiable simulation and rendering into robot manipulation learning. And Zhu et al. [57] present contact-aware model-based learning from visual demonstration for robotic manipulation via differentiable simulation and rendering. While utilizing differentiable physics simulation to generate robot manipulation trajectories has become a popular research topic recently, many of these works still rely on hand-crafted reward functions, which is not optimal [25, 28, 29]. In this paper, we propose combining differentiable physics simulation, differentiable rendering, and a vision-language model for specifying reward functions based on text-based task instructions.

C. Reward Learning

Reward learning is crucial for robot learning methods such as reinforcement learning [9, 12, 44]. A well-designed reward function can significantly improve performance and learning efficiency, whereas a poorly designed one may hinder progress. Traditionally, reward design has often relied on manual trial-and-error methods. However, recently, inferring reward functions from text-based instructions using large language models has gained popularity [18, 33, 50, 55]. For instance, Ma et al. [33] has demonstrated the ability to achieve human-level reward design through coding language models, with algorithms capable of analyzing trained policy feedback to fine-tune reward functions. Another approach involves learning reward functions from demonstrations [2, 10, 15, 31, 37]. Ma et al. [31] presented a self-supervised pretrained visual representation, enabling the generation of reward functions for unseen robotic tasks based on this pretrained representation. To enable cross-modal reward learning [32, 41, 46], Ma et al. [32] introduced a unified objective for vision-language representation and reward learning from demonstrations with text annotations, training multi-modal representations to serve as reward functions across language and image domains. In this paper, we integrate the cross-modal reward learning method with differentiable physics simulation and rendering to generate robot demonstrations.

III. TECHNICAL APPROACH

A. Overview

Given a robot manipulation task, where the task goal \mathcal{G} is specified by a text-based instruction l , which can be generated

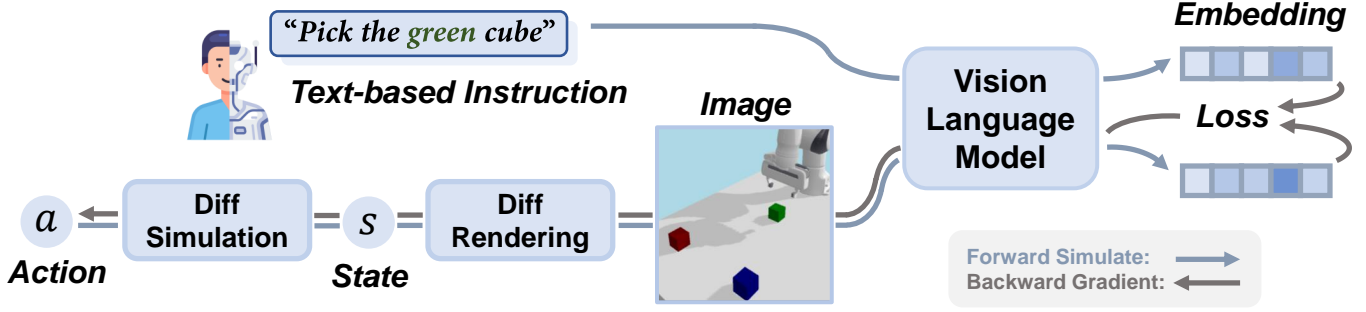


Fig. 2. The overall pipeline of our proposed DiffGen. Our system first initiates action sequences, simulates the state changes, and renders visual observations after manipulation, via differentiable simulation and differentiable rendering. Then, a vision-language model is employed to measure the distance between the visual observations and the text-based instructions. Thanks to the differentiability of each component, feasible action sequences can be generated by gradient descent optimization.

by a language model [1] or provided by a human, the problem addressed in this paper is robot demonstration generation. The objective is to find a sequence of actions $\{a_t\}_{t=0}^T$ that control the robot to modify the state s_t to reach a final goal state s^G that satisfies the instruction l . Specifically, we aim to maximize the following objectives:

$$\begin{aligned} \max_{a_t} \mathbb{E} \left[\sum_{t=0}^T \gamma^t \mathcal{R}(s_t, a_t; \mathcal{G}) \right], \\ \text{s.t. } s_{t+1} = \mathcal{T}(s_t, a_t), s_t \in \mathcal{S}, a_t \in \mathcal{A}, \end{aligned} \quad (1)$$

where \mathcal{S} denotes the state space, \mathcal{A} denotes the action space, $\mathcal{T} : \mathcal{S} \times \mathcal{A} \rightarrow \mathcal{S}$ is the transition map, and \mathcal{R} is the goal-conditioned reward function.

Our proposed approach, as shown in Fig. 2, leverages recent advances in differentiable physics simulation, differentiable rendering, and vision-language pretraining to optimize an action sequence $\{a_t\}_{t=0}^T$ that achieves the goal \mathcal{G} . In the following sections, we will describe how to utilize the differentiable physics simulation and rendering to model the environment dynamics (Sec. III-B), how to achieve goal specification via a vision-language model (Sec. III-C), and how to generate actions via an optimization-based method (Sec. III-D).

B. Differentiable Physics-based Simulation and Rendering

With an action sequence $\{a_t\}_{t=0}^T$, a physics-based simulation $f(\cdot, \cdot)$ takes the current state s_t and action a_t to calculate the next state s_{t+1} via a forward dynamic function:

$$s_{t+1} = f(s_t, a_t). \quad (2)$$

When the forward function is formulated in a differentiable manner [51, 54], the gradients of the next state with respect to the current state $\frac{\partial s_{t+1}}{\partial s_t}$ and with respect to the action $\frac{\partial s_{t+1}}{\partial a_t}$ can be obtained through back-propagation.

$$\begin{aligned} \frac{\partial s_{t+1}}{\partial s_t} &= \frac{\partial f(s_t, a_t)}{\partial s_t}, \\ \frac{\partial s_{t+1}}{\partial a_t} &= \frac{\partial f(s_t, a_t)}{\partial a_t}. \end{aligned} \quad (3)$$

Previous work has optimized action sequences that transition the environment to the goal state via gradient descent [28].

However, the goal state is usually directly specified by a human or determined by a hand-crafted objective function, which is labor-intensive. In our proposed method, we aim to specify the goal state via a pretrained vision-language model. Therefore, our next step is to generate the visual observation $\mathcal{I} \in \mathbb{R}^{H \times W \times 3}$ using a renderer $g(\cdot)$, where \mathcal{I} is an RGB image with height H and width W :

$$\mathcal{I}_t = g(s_t). \quad (4)$$

In practice, the state s_t comprises the transformation pose of each object \mathcal{O}_i in the scene. We transform each object to its simulated pose to generate the visual observation that describes the current state. And when the renderer is also differentiable [24], the gradient of each pixel on the image \mathcal{I} with respect to the state $\frac{\partial \mathcal{I}}{\partial s_t}$ is also available:

$$\frac{\partial \mathcal{I}}{\partial s_t} = \frac{\partial g(s_t)}{\partial s_t}. \quad (5)$$

Now, the proposed system enables us to achieve goal specification in the visual observation space.

C. Goal Specification via Vision-Language Model

Goal specification is a crucial step in robot demonstration generation, involving the assessment of whether the current state aligns with the provided task instruction. To achieve this, given a text-based instruction l , we utilize a vision-language model $h(\cdot)$, which is pretrained for value learning (for more details, please refer to LIV [32]), to encode the instruction:

$$z^l = h(l), \quad (6)$$

while the visual observation \mathcal{I} could be also encoded via:

$$z^{\mathcal{I}} = h(\mathcal{I}). \quad (7)$$

When the action sequence transitions the environment to a state s_t that fulfills the task instruction l , the distance between the embedding vector of the text-based instruction z^l and the embedding vector of the visual observation $z^{\mathcal{I}}$ should be minimized. So the objective function $\mathcal{L}(\cdot, \cdot)$ under the setting of our proposed system is:

$$\mathcal{L}(z^l, z^{\mathcal{I}}) = -\frac{z^l \cdot z^{\mathcal{I}}}{\|z^l\| \|z^{\mathcal{I}}\|}. \quad (8)$$

D. Robot Demonstration Generation via Optimization

To generate the robot demonstration, the system aims to find a robot action sequence $\{a_t\}_{t=0}^T$ that can change the environment state to s^G , such that the rendered visual observation \mathcal{I} has a similar embedding vector $z^{\mathcal{I}}$ to the embedding vector of the text-based task instruction z^l . Previous works typically train a policy network via model-free reinforcement learning with the assistance of a reward function, which suffers from poor sample efficiency. In our proposed system, thanks to the differentiability of the physics simulation, rendering, and the neural-network-based vision-language model, we can directly backpropagate the gradient and search for feasible action sequences that minimize the objective function \mathcal{L} via gradient descent:

$$\{a_t\}_{t=0}^T \leftarrow \{a_t\}_{t=0}^T - \lambda \frac{\partial \mathcal{L}}{\partial \{a_t\}_{t=0}^T}, \quad (9)$$

$$\frac{\partial \mathcal{L}}{\partial \{a_t\}_{t=0}^T} = \frac{\partial \mathcal{L}}{\partial z^{\mathcal{I}}} \frac{\partial z^{\mathcal{I}}}{\partial \mathcal{I}} \frac{\partial \mathcal{I}}{\partial s_T} \frac{\partial s_T}{\partial \{a_t\}_{t=0}^T}, \quad (10)$$

where the λ is the optimization step size. With this optimization-based demonstration generation, the system could generate robot data effectively and efficiently.

As mentioned in studies [8, 42], previous optimization methods based on differentiable physics simulation often suffer from gradient vanishing or explosion, likely to get stuck in local minima. This is because the gradients from the objectives have to be backpropagated through the entire sequence of state transitions, which may lead to error accumulation and gradient instability.

To address this issue, we design a novel optimization strategy to decompose the long-horizon trajectory into a series of short-horizon episodes. Each short episode is optimized individually, one by one, with a higher learning rate and lower optimization steps to enable fast exploration. The cumulative trajectory keeps expanding until the objective function reaches the extreme or the iteration number reaches the limit, at which point the process is automatically stopped.

IV. EXPERIMENTS

In this section, we introduce the implementation details of the proposed system and the experimental setup of this paper. We conduct experiments to evaluate the efficiency and performance of the proposed system.

A. Implementation Details

1) *Differentiable Physics Simulation*: In our experiments, we use the differentiable physics simulator NimblePhysics [51] as our simulation backend. NimblePhysics provides Jacobians of the environment dynamics while supporting collision handling simultaneously. This is achieved by solving the Linear Complementarity Problems (LCPs). Most of the computationally intensive parts of the simulation are implemented in C++ for high performance. For more details, please refer to [51].

2) *Differentiable Renderer*: We replace the default rendering module of NimblePhysics with a differentiable renderer, Redner [24], to enable the end-to-end differentiability of the entire pipeline. We use the fast deferred rendering mode of Redner to ensure correct gradient estimation, fast backpropagation speed, and high-quality rendering results. For more details, please refer to [24].

The output state of NimblePhysics, which is represented in joint space, is converted to a list of transformation matrices to meet the input requirements of Redner. Those transformation matrices describe the absolute positions and orientations of all simulated links in Cartesian space. We implement this conversion in a differentiable manner to avoid breaking the gradient flow.

3) *Vision-Language Model*: The vision-language representation model used in our experiments is LIV [32], a CLIP-style model with ResNet-50 [13] as its vision backbone and DistilBERT [43] as its language encoder. The model is initialized with weights from CLIP [41] and pretrained on EpicKitchen [3], which is a large-scale first-person non-robotic video dataset, consisting of human daily activities in the kitchen, annotated with natural language descriptions. The pretrained models are also fine-tuned with robot data to reduce the domain gap. We fine-tune the vision encoder with a learning rate of $1e-5$ and a batch size of 64 following the default setting in LIV. The language encoder is frozen during fine-tuning. The fine-tuned encoders are then used to extract features and construct rewards. We exclusively utilize a restricted scale of data around 400k. In Sec. IV-D, we demonstrate that the model’s performance is not overfitting on this dataset.

4) *Gradient-based Optimization*: To perform gradient-based optimization on the actions, we use the AdamW optimizer with a learning rate of $1e-2$ for most tasks. For the fixed-horizon strategy, the optimization steps and horizon lengths are decided according to the complexity of each task.

B. Task Setup

As shown in Fig. 3, we design three tasks to demonstrate the performance of our method. All these tasks are evaluated in simulation on a Franka Emika Panda robot arm. The arm is equipped with a default gripper, placed on a square platform, and initialized with random end-effector positions. Though we use Franka Emika Panda in most cases, our method is general and can be applied to other robot embodiments, such as UR5e, as will be demonstrated in Sec. IV-D.

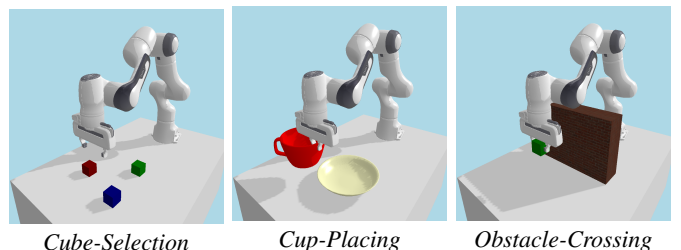


Fig. 3. Visualization of the tasks, generated by the PyBullet renderer.

Specifically, these tasks are:

1) *Cube-Selection*: The job is to distinguish the cube in the target color and select it. Cubes of different colors (red, blue, green) are placed on the platform at random positions. Given a brief language instruction, such as "grasp the red cube", the robot is expected to move its gripper to the target cube. We consider the task successful if the gripper is within a certain distance above the target cube. The deviation threshold is set to 10cm. To handle this task, we optimize the robot trajectory for 200 steps with a fixed horizon of 50 timesteps.

2) *Cup-Placing*: The job is to place a cup onto the dish. The cup is already held by the robot arm and the dish is placed on the platform at a random position. The robot is instructed to "put the cup on the dish". The task is considered successful if the cup is accurately put inside the dish in the final state, which is measured by the distance between the cup bottom and the dish surface. After scrutinizing the cup and dish at different relative positions, we set the threshold to 5cm, since 5cm is much smaller than the radius of the dish, indicating the center of the cup bottom is inside the dish. The optimization process is set to 200 steps and the horizon is set to 70 timesteps in this case. Since it is a task that requires precise manipulation, we decrease the learning rate to $1e-3$ to ensure the stability of the optimization process.

3) *Obstacle-Crossing*: The job is to move the cube to the commanded position while avoiding the obstacle. The obstacle is implemented as a wall located between the initial and the target place. The size of the wall is $30cm \times 40cm \times 10cm$. The commands can be "move to the left side of the wall", "move to the right side of the wall", or "move to the back of the wall". The task is considered successful if the robot crosses the obstacle and reaches the target position. For example, if the command is "move to the back of the wall" and the cube on the robot hand is delivered to the $40cm \times 30cm$ region behind the wall, we consider the task a success. We set the optimization steps to 300 and the horizon length to 100.

C. Evaluating the Efficiency and Accuracy

1) *Robot Demonstration Generation*: We show that our method is capable of generating high-quality robot demonstrations on all three tasks. To this end, we set up 100 randomly initialized environments for each task and apply our method to those environments. Each trajectory is optimized individually for a predefined number of steps with a fixed horizon. The optimal trajectory can be considered as either the one with the highest reward during the whole optimization process, denoted as *Ours (best traj.)*; or the last trajectory, denoted as *Ours (last traj.)*. The performance of our method is evaluated based on the collected trajectories, averaged over all environments.

We present the loss curves of our method in Fig. 4, Fig. 5, and Fig. 6. The left column shows the trajectory-level losses with respect to the optimization steps. As we can see, the loss decreases steadily and converges rapidly as the optimization process proceeds. The convergence is achieved within a few hundred steps, indicating the efficiency of our method. The

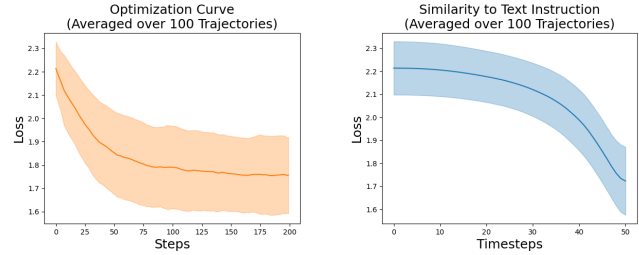


Fig. 4. Loss Curves on Cube-Selection Task

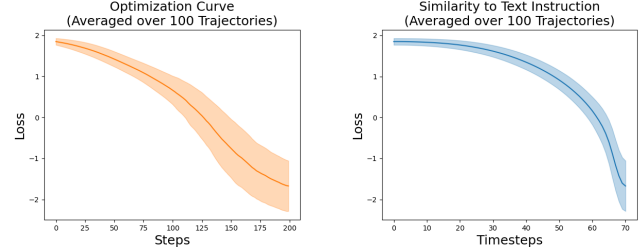


Fig. 5. Loss Curves on Cup-Placing Task

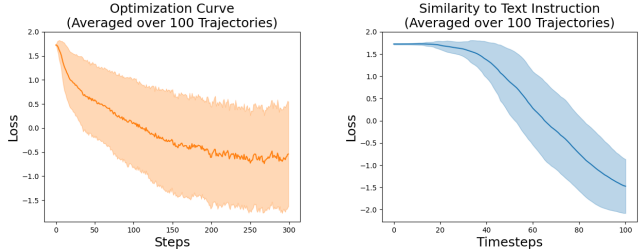


Fig. 6. Loss Curves on Obstacle-Crossing Task

right column shows the loss curves of those optimized trajectories. The loss can be regarded as the embedding distance between the current observation and the text instruction. As time goes by, the loss keeps decreasing, suggesting that the robot is approaching the goal. The robot stops at a state with relatively low loss. This indicates the potential of our method in generating smooth and accurate robot demonstrations.

2) *Comparison with Reinforcement Learning Baselines*: A popular way to generate robot demonstrations is to train a reinforcement learning agent with reward functions generated from vision-language models (VLMs) or large language models (LLMs). We choose two representative paradigms from past works as our baselines [33, 46].

- *VLM-based Methods*, which train a PPO agent with a trajectory-level reward generated by some vision-language model, such as S3D [53]. We follow the implementation in RoboCLIP [46] to construct the reward as the similarity score between the task descriptor and the observed agent behaviors. We replace the original S3D model with fine-tuned LIV in our experiments to ensure a fair comparison. Apart from the cosine similarity, we also set up a baseline that uses the InfoNCE [38] loss as the reward function. Those two baselines are denoted as *PPO-CosSim* and *PPO-InfoNCE*, respectively.
- *LLM-based Methods*, which obtain the reward function from some large language models with code-writing capabilities, such as GPT-4 [1]. The entire environment of

the task, along with natural language prompts, is fed into those LLMs to generate codes of reward functions, which are then embedded into the PPO training pipeline. We follow the prompt designs in Eureka [33] and keep the reward reflection approach proposed in that work. This baseline is denoted as *PPO-LLM*.

We compare our method to the baselines in terms of the success rate, mean deviation of the final position from the target, and the total optimization steps. For both baselines, we first train the agents using the PPO algorithm. The trained policies are then evaluated on 100 trajectories to obtain an average performance. The results are shown in Table I.

TABLE I
QUANTITATIVE RESULTS ON CUBE-SELECTION TASK

| Method | Success Rate | Deviation | Tot. Opt. Steps |
|------------------------|--------------|-----------|-----------------|
| Ours (best traj.) | 0.85 | 0.082 | 20k |
| Ours (last traj.) | 0.81 | 0.095 | 20k |
| PPO-CosSim | 0.06 | 0.446 | 10M |
| PPO-InfoNCE | 0.00 | 0.259 | 10M |
| PPO-LLM (first iter.) | 0.25 | 0.274 | 5M |
| PPO-LLM (second iter.) | 0.37 | 0.173 | 5M |
| PPO-LLM (third iter.) | 0.40 | 0.224 | 5M |

Our method outperforms all baselines and achieves a relatively high success rate with lower computation costs. Simply applying LIV-generated rewards to PPO training, as demonstrated in *PPO-CosSim* and *PPO-InfoNCE*, fails to learn a reasonable policy. It indicates that, by directly backpropagating the gradients of visual feedback to the action space, our method achieves higher sample efficiency compared to RL baselines.

D. Evaluating the Generalizability

Robot data is known as expensive to collect and hard to be reused. Human data, on the other hand, is easy to scale up while facing severe domain gaps. To bridge the gap between humans and robots, we use some robotic data to fine-tune the vision-language model after pretraining it on human data. We argue that the model is not overfitted to those robotic data and can be generalized to new embodiments or scenarios. We conduct the following experiments to demonstrate this:

1) *Zero-shot Goal Specification*: We conduct evaluations on the Obstacle-Crossing task. The vision-language model for reward specification is trained on the human data from EpicKitchen only, without any fine-tuning. We set the language instructions to be "move to the left side of the wall" or "move to the right side of the wall", and expect the robot to be optimized to move left or right accordingly. The success is defined as the cube ending up with a positive horizontal displacement if commanded left, and negative if commanded right. This is challenging since the robot has never encountered any robotic data before, and can only infer the concept of "left" and "right" from human videos. The results are shown in Table II, from which we can see that most of the time the robot can tell left from right and move accordingly, indicating the potential

of our method in transferring human demonstrations to robot tasks.

TABLE II
ZERO-SHOT GOAL SPECIFICATION ON OBSTACLE-CROSSING TASK

| Command | Success Rate | Displacement | Final Position |
|------------|--------------|--------------|----------------|
| Move Left | 0.978 | -0.205 | -0.217 |
| Move Right | 0.704 | 0.049 | 0.050 |

2) *Cross-Embodiment Transfer and Generalization*: To evaluate the performance of the proposed method on the unseen robotic embodiment, we conduct experiments on the Cup-Placing task. We first fine-tune the vision-language model with data from Panda Emika Franka and then evaluate its performance on a UR5e robot. The challenge in this experiment lies in the embodiment gap between those two robots. To successfully place the cup onto the dish, the robot needs to realize that the concepts of "put" and "on" are invariant across different embodiments and associate the language instructions with the consequences of its actions, rather than embodiment-specific behaviors. Apart from the cross-embodiment transfer experiment, we also evaluate whether the robot can learn from demonstrations of different scenarios and generalize to a new one. To this end, we change the color of the cup during evaluation. The color is unseen during the fine-tuning process. Since the color of the manipulated object is irrelevant to the language instructions in this case, the robot is expected to behave the same. The results are shown in Table III. As we can see, with little performance drop, the robot is able to generalize to the novel embodiment and the novel scenario.

TABLE III
GENERALIZATION ON CUP-PLACING TASK

| Scenario | Success Rate | Deviation |
|--|--------------|-----------|
| Same embodiment, seen color (baseline) | 0.87 | 0.0287 |
| Same embodiment, unseen color | 0.53 | 0.0553 |
| Novel embodiment, seen color | 0.84 | 0.0535 |

E. Ablation Study

In this section, we conduct two ablation studies to investigate the effectiveness of our optimization strategy and the vision-language goal specification.

- We first change the episodic optimization strategy to a fixed-horizon single-iteration optimization. The robot trajectory is optimized for 300 steps with a preset horizon of 100 timesteps. The setting is denoted as *Ours (w/o ep. opt.)*.
- We also remove the differentiable rendering module and set up a baseline that uses hand-crafted rewards conditioned on privileged information rather than the rendered visual observation, denoted as *Handcraft (w/o diff. render)*.

As shown in Table IV, both ablations lead to a significant drop in success rate compared to the original method. With

TABLE IV
ABLATIONS ON OBSTACLE-CROSSING TASK

| Method | Success Rate | Tot. Opt. Steps |
|------------------------------|--------------|-----------------|
| Ours | 0.72 | 23.9k |
| Ours (w/o ep. opt.) | 0.41 | 30k |
| Handcraft (w/o diff. render) | 0.19 | 30k |

the episodic optimization strategy, our method is capable of handling long trajectory optimization problems, achieving superior performance while consuming fewer optimization steps.

The integration of differentiable rendering and vision-language models is also crucial for the success of our method. Compared to the baseline using hand-crafted rewards, our method demonstrates the capability of avoiding local minima. This is because the vision-language model can provide more informative feedback associated with task progress. A well-trained vision-language model can guide the robot out of local minima and towards the goal, leading to better performance.

V. LIMITATION AND FUTURE WORK

Though our approach shows promising results in generating robot demonstrations with action annotations, we recognize that its performance is still limited by the quality of the employed vision-language model. Currently, we fine-tune the model using some action-free robotic videos to reduce the domain gap between human data pretraining and robot tasks, as suggested. We believe the need for robotic fine-tuning can be alleviated with a more advanced vision-language model. Our approach can benefit from future advances in representation learning and vision-language pretraining, thus able to be extended to more complex tasks and scenarios.

VI. CONCLUSION

In this paper, we validate the feasibility of integrating differentiable physics simulation, differentiable rendering, and a vision-language model for automatic and efficient robot demonstration generation in simulation. Given a simulated robot manipulation scenario, our proposed system initiates a sequence of manipulation actions, simulates the manipulation results, and renders the visual observation after manipulation. With a pretrained vision-language model, our system can measure the discrepancy between the observation after manipulation and the text-based task instruction. Thanks to the differentiability of each component, we can directly optimize the action sequence via gradient descent to achieve the instruction. We believe that with the proposed approach to efficiently generating robot demonstrations in simulation and the recent progress in robot simulation task generation, we have the opportunity to scale up robot data for future research.

REFERENCES

[1] Josh Achiam, Steven Adler, Sandhini Agarwal, Lama Ahmad, Ilge Akkaya, Florencia Leoni Aleman, Diogo Almeida, Janko Altmenschmidt, Sam Altman, Shyamal Anadkat, et al. Gpt-4 technical report. *arXiv preprint arXiv:2303.08774*, 2023.

[2] Chethan Bhateja, Derek Guo, Dibya Ghosh, Anikait Singh, Manan Tomar, Quan Vuong, Yevgen Chebotar, Sergey Levine, and Aviral Kumar. Robotic offline rl from internet videos via value-function pre-training. *arXiv preprint arXiv:2309.13041*, 2023.

[3] Dima Damen, Hazel Doughty, Giovanni Maria Farinella, Antonino Furnari, Jian Ma, Evangelos Kazakos, Davide Moltisanti, Jonathan Munro, Toby Perrett, Will Price, and Michael Wray. Rescaling egocentric vision: Collection, pipeline and challenges for epic-kitchens-100. *International Journal of Computer Vision (IJCV)*, 130:33–55, 2022. URL <https://doi.org/10.1007/s11263-021-01531-2>.

[4] Filipe de Avila Belbute-Peres, Kevin Smith, Kelsey Allen, Josh Tenenbaum, and J Zico Kolter. End-to-end differentiable physics for learning and control. *Advances in neural information processing systems*, 31, 2018.

[5] Jonas Degraeve, Michiel Hermans, Joni Dambre, et al. A differentiable physics engine for deep learning in robotics. *Frontiers in neurorobotics*, 13:406386, 2019.

[6] Jacob Devlin, Ming-Wei Chang, Kenton Lee, and Kristina Toutanova. Bert: Pre-training of deep bidirectional transformers for language understanding. *arXiv preprint arXiv:1810.04805*, 2018.

[7] Yilun Du, Sherry Yang, Bo Dai, Hanjun Dai, Ofir Nachum, Josh Tenenbaum, Dale Schuurmans, and Pieter Abbeel. Learning universal policies via text-guided video generation. *Advances in Neural Information Processing Systems*, 36, 2024.

[8] C. Daniel Freeman, Erik Frey, Anton Raichuk, Sertan Girgin, Igor Mordatch, and Olivier Bachem. Brax - a differentiable physics engine for large scale rigid body simulation, 2021. URL <http://github.com/google/brax>.

[9] Scott Fujimoto, Herke Hoof, and David Meger. Addressing function approximation error in actor-critic methods. In *International conference on machine learning*, pages 1587–1596. PMLR, 2018.

[10] Dibya Ghosh, Chethan Anand Bhateja, and Sergey Levine. Reinforcement learning from passive data via latent intentions. In *International Conference on Machine Learning*, pages 11321–11339. PMLR, 2023.

[11] Ian Goodfellow, Jean Pouget-Abadie, Mehdi Mirza, Bing Xu, David Warde-Farley, Sherjil Ozair, Aaron Courville, and Yoshua Bengio. Generative adversarial networks. *Communications of the ACM*, 63(11): 139–144, 2020.

[12] Tuomas Haarnoja, Aurick Zhou, Pieter Abbeel, and Sergey Levine. Soft actor-critic: Off-policy maximum entropy deep reinforcement learning with a stochastic actor. In *International conference on machine learning*, pages 1861–1870. PMLR, 2018.

[13] Kaiming He, Xiangyu Zhang, Shaoqing Ren, and Jian Sun. Deep residual learning for image recognition. In *Proceedings of the IEEE conference on computer vision and pattern recognition*, pages 770–778, 2016.

[14] Kaiming He, Georgia Gkioxari, Piotr Dollár, and Ross Girshick. Mask r-cnn. In *Proceedings of the IEEE international conference on computer vision*, pages 2961–2969, 2017.

[15] Jonathan Ho and Stefano Ermon. Generative adversarial imitation learning. *Advances in neural information processing systems*, 29, 2016.

[16] Taylor A Howell, Simon Le Cleac’h, J Zico Kolter, Mac Schwager, and Zachary Manchester. Dojo: A differentiable simulator for robotics. *arXiv preprint arXiv:2203.00806*, 9, 2022.

[17] Wenlong Huang, Chen Wang, Ruohan Zhang, Yunzhu Li, Jiajun Wu, and Li Fei-Fei. Voxposer: Composable 3d value maps for robotic manipulation with language models. In *Towards Generalist Robots: Learning Paradigms for Scalable Skill Acquisition@ CoRL2023*, 2023.

[18] Zhiao Huang, Feng Chen, Yewen Pu, Chunru Lin, Hao Su, and Chuang Gan. Diffvl: Scaling up soft body manipulation using vision-language driven differentiable physics. *Advances in Neural Information Processing Systems*, 36, 2024.

[19] Krishna Murthy Jatavallabhula, Miles Macklin, Florian Golemo, Vikram Voleti, Linda Petrini, Martin Weiss, Brendan Considine, Jerome Parent-Levesque, Kevin Xie, Kenny Erleben, Liam Paull, Florian Shkurti, Derek Nowrouzezahrai, and Sanja Fidler. gradsim: Differentiable simulation for system identification and visuomotor control. *International Conference on Learning Representations (ICLR)*, 2021. URL https://openreview.net/forum?id=c_E8kFWfhp0.

[20] Pushkal Katara, Zhou Xian, and Katerina Fragkiadaki. Gen2sim: Scaling up robot learning in simulation with generative models. *arXiv preprint arXiv:2310.18308*, 2023.

[21] Hiroharu Kato, Deniz Beker, Mihai Morariu, Takahiro Ando, Toru Matsuoka, Wadim Kehl, and Adrien Gaidon. Differentiable rendering:

- A survey. *arXiv preprint arXiv:2006.12057*, 2020.
- [22] Alexander Kirillov, Eric Mintun, Nikhila Ravi, Hanzi Mao, Chloe Rolland, Laura Gustafson, Tete Xiao, Spencer Whitehead, Alexander C Berg, Wan-Yen Lo, et al. Segment anything. In *Proceedings of the IEEE/CVF International Conference on Computer Vision*, pages 4015–4026, 2023.
- [23] Sizhe Li, Zhiao Huang, Tao Chen, Tao Du, Hao Su, Joshua B Tenenbaum, and Chuang Gan. Dexdeform: Dexterous deformable object manipulation with human demonstrations and differentiable physics. *arXiv preprint arXiv:2304.03223*, 2023.
- [24] Tzu-Mao Li, Miika Aittala, Frédo Durand, and Jaakko Lehtinen. Differentiable monte carlo ray tracing through edge sampling. *ACM Trans. Graph. (Proc. SIGGRAPH Asia)*, 37(6):222:1–222:11, 2018.
- [25] Xingyu Lin, Zhiao Huang, Yunzhu Li, Joshua B Tenenbaum, David Held, and Chuang Gan. DiffSkill: Skill abstraction from differentiable physics for deformable object manipulations with tools. *arXiv preprint arXiv:2203.17275*, 2022.
- [26] Ruoshi Liu, Rundi Wu, Basile Van Hoorick, Pavel Tokmakov, Sergey Zakharov, and Carl Vondrick. Zero-1-to-3: Zero-shot one image to 3d object. In *Proceedings of the IEEE/CVF International Conference on Computer Vision*, pages 9298–9309, 2023.
- [27] Shichen Liu, Tianye Li, Weikai Chen, and Hao Li. Soft rasterizer: A differentiable renderer for image-based 3d reasoning. In *Proceedings of the IEEE/CVF international conference on computer vision*, pages 7708–7717, 2019.
- [28] Jun Lv, Qiaojun Yu, Lin Shao, Wenhai Liu, Wenqiang Xu, and Cewu Lu. Sagci-system: Towards sample-efficient, generalizable, compositional, and incremental robot learning. In *2022 International Conference on Robotics and Automation (ICRA)*, pages 98–105. IEEE, 2022.
- [29] Jun Lv, Yunhai Feng, Cheng Zhang, Shuang Zhao, Lin Shao, and Cewu Lu. Sam-rl: Sensing-aware model-based reinforcement learning via differentiable physics-based simulation and rendering. *Proceedings of Robotics: Science and Systems (RSS)*, 2023.
- [30] Pingchuan Ma, Tao Du, Joshua B Tenenbaum, Wojciech Matusik, and Chuang Gan. Risp: Rendering-invariant state predictor with differentiable simulation and rendering for cross-domain parameter estimation. In *International Conference on Learning Representations*, 2021.
- [31] Yecheng Jason Ma, Shagun Sodhani, Dinesh Jayaraman, Osbert Bastani, Vikash Kumar, and Amy Zhang. Vip: Towards universal visual reward and representation via value-implicit pre-training. *arXiv preprint arXiv:2210.00030*, 2022.
- [32] Yecheng Jason Ma, Vikash Kumar, Amy Zhang, Osbert Bastani, and Dinesh Jayaraman. Liv: Language-image representations and rewards for robotic control. In *International Conference on Machine Learning*, pages 23301–23320. PMLR, 2023.
- [33] Yecheng Jason Ma, William Liang, Guanzhi Wang, De-An Huang, Osbert Bastani, Dinesh Jayaraman, Yuke Zhu, Linxi Fan, and Anima Anandkumar. Eureka: Human-level reward design via coding large language models. In *The Twelfth International Conference on Learning Representations*, 2023.
- [34] Viktor Makoviychuk, Lukasz Wawrzyniak, Yunrong Guo, Michelle Lu, Kier Storey, Miles Macklin, David Hoeller, Nikita Rudin, Arthur Allshire, Ankur Handa, et al. Isaac gym: High performance gpu-based physics simulation for robot learning. *arXiv preprint arXiv:2108.10470*, 2021.
- [35] Ajay Mandlekar, Danfei Xu, Josiah Wong, Soroush Nasiriany, Chen Wang, Rohun Kulkarni, Li Fei-Fei, Silvio Savarese, Yuke Zhu, and Roberto Martín-Martín. What matters in learning from offline human demonstrations for robot manipulation. *arXiv preprint arXiv:2108.03298*, 2021.
- [36] Ajay Mandlekar, Soroush Nasiriany, Bowen Wen, Iretyayo Akinola, Yashraj Narang, Linxi Fan, Yuke Zhu, and Dieter Fox. Mimicgen: A data generation system for scalable robot learning using human demonstrations. In *Towards Generalist Robots: Learning Paradigms for Scalable Skill Acquisition@ CoRL2023*, 2023.
- [37] Suraj Nair, Aravind Rajeswaran, Vikash Kumar, Chelsea Finn, and Abhinav Gupta. R3m: A universal visual representation for robot manipulation. *arXiv preprint arXiv:2203.12601*, 2022.
- [38] Aaron van den Oord, Yazhe Li, and Oriol Vinyals. Representation learning with contrastive predictive coding. *arXiv preprint arXiv:1807.03748*, 2018.
- [39] Ben Poole, Ajay Jain, Jonathan T Barron, and Ben Mildenhall. Dream-fusion: Text-to-3d using 2d diffusion. In *The Eleventh International Conference on Learning Representations*, 2022.
- [40] Yi-Ling Qiao, Junbang Liang, Vladlen Koltun, and Ming C Lin. Scalable differentiable physics for learning and control. *arXiv preprint arXiv:2007.02168*, 2020.
- [41] Alec Radford, Jong Wook Kim, Chris Hallacy, Aditya Ramesh, Gabriel Goh, Sandhini Agarwal, Girish Sastry, Amanda Askell, Pamela Mishkin, Jack Clark, et al. Learning transferable visual models from natural language supervision. In *International conference on machine learning*, pages 8748–8763. PMLR, 2021.
- [42] Jiawei Ren, Cunjun Yu, Siwei Chen, Xiao Ma, Liang Pan, and Ziwei Liu. Diffmimic: Efficient motion mimicking with differentiable physics. *arXiv preprint arXiv:2304.03274*, 2023.
- [43] Victor Sanh, Lysandre Debut, Julien Chaumond, and Thomas Wolf. Distilbert, a distilled version of bert: smaller, faster, cheaper and lighter. *arXiv preprint arXiv:1910.01108*, 2019.
- [44] John Schulman, Filip Wolski, Prafulla Dhariwal, Alec Radford, and Oleg Klimov. Proximal policy optimization algorithms. *arXiv preprint arXiv:1707.06347*, 2017.
- [45] Yang Song, Jascha Sohl-Dickstein, Diederik P Kingma, Abhishek Kumar, Stefano Ermon, and Ben Poole. Score-based generative modeling through stochastic differential equations. *arXiv preprint arXiv:2011.13456*, 2020.
- [46] Sumedh Sontakke, Jesse Zhang, Séb Arnold, Karl Pertsch, Erdem Bıyık, Dorsa Sadigh, Chelsea Finn, and Laurent Itti. Roboclip: One demonstration is enough to learn robot policies. *Advances in Neural Information Processing Systems*, 36, 2024.
- [47] Emanuel Todorov, Tom Erez, and Yuval Tassa. Mujoco: A physics engine for model-based control. In *2012 IEEE/RSJ international conference on intelligent robots and systems*, pages 5026–5033. IEEE, 2012.
- [48] Ashish Vaswani, Noam Shazeer, Niki Parmar, Jakob Uszkoreit, Llion Jones, Aidan N Gomez, Łukasz Kaiser, and Illia Polosukhin. Attention is all you need. *Advances in neural information processing systems*, 30, 2017.
- [49] Lirui Wang, Yiyang Ling, Zhecheng Yuan, Mohit Shridhar, Chen Bao, Yuzhe Qin, Bailin Wang, Huazhe Xu, and Xiaolong Wang. Gensim: Generating robotic simulation tasks via large language models. In *The Twelfth International Conference on Learning Representations*, 2023.
- [50] Yufei Wang, Zhou Xian, Feng Chen, Tsun-Hsuan Wang, Yian Wang, Katerina Fragkiadaki, Zackory Erickson, David Held, and Chuang Gan. Robogen: Towards unleashing infinite data for automated robot learning via generative simulation. *arXiv preprint arXiv:2311.01455*, 2023.
- [51] Keenon Werling, Dalton Omens, Jeongseok Lee, Ioannis Exarchos, and C Karen Liu. Fast and feature-complete differentiable physics for articulated rigid bodies with contact. *arXiv preprint arXiv:2103.16021*, 2021.
- [52] Fanbo Xiang, Yuzhe Qin, Kaichun Mo, Yikuan Xia, Hao Zhu, Fangchen Liu, Minghua Liu, Hanxiao Jiang, Yifu Yuan, He Wang, et al. Sapien: A simulated part-based interactive environment. In *Proceedings of the IEEE/CVF conference on computer vision and pattern recognition*, pages 11097–11107, 2020.
- [53] Saining Xie, Chen Sun, Jonathan Huang, Zhuowen Tu, and Kevin Murphy. Rethinking spatiotemporal feature learning: Speed-accuracy trade-offs in video classification. In *Proceedings of the European conference on computer vision (ECCV)*, pages 305–321, 2018.
- [54] Gang Yang, Siyuan Luo, and Lin Shao. Jade: A differentiable physics engine for articulated rigid bodies with intersection-free frictional contact. *arXiv preprint arXiv:2309.04710*, 2023.
- [55] Wenhao Yu, Nimrod Gileadi, Chuyuan Fu, Sean Kirmani, Kuang-Huei Lee, Montse Gonzalez Arenas, Hao-Tien Lewis Chiang, Tom Erez, Leonard Hasenclever, Jan Humplik, et al. Language to rewards for robotic skill synthesis. *arXiv preprint arXiv:2306.08647*, 2023.
- [56] Shuang Zhao, Wenzel Jakob, and Tzu-Mao Li. Physics-based differentiable rendering: from theory to implementation. In *ACM siggraph 2020 courses*, pages 1–30. 2020.
- [57] Xinghao Zhu, Jinghan Ke, Zhixuan Xu, Zhixin Sun, Bizhe Bai, Jun Lv, Qingtao Liu, Yuwei Zeng, Qi Ye, Cewu Lu, Masayoshi Tomizuka, and Lin Shao. Diff-rlfd: Contact-aware model-based learning from visual demonstration for robotic manipulation via differentiable physics-based simulation and rendering. In *Conference on Robot Learning (CoRL)*, 2023.